Development 135, 4165-4177 (2008) doi:10.1242/dev.026633

Competence, specification and commitment to an olfactory placode fate

Sujata Bhattacharyya and Marianne Bronner-Fraser*

The nasal placode shares a common origin with other sensory placodes within a pre-placodal domain at the cranial neural plate border. However, little is known about early events in nasal placode development as it segregates from prospective lens, neural tube and epidermis. Here, Dlx3, Dlx5, Pax6 and the pan-neuronal marker Hu serve as molecular labels to follow the maturation of olfactory precursors over time. When competence to form olfactory placode was tested by grafting ectoderm from different axial levels to the anterior neural fold, we found that competence is initially broad for head, but not trunk, ectoderm and declines rapidly with time. Isolated olfactory precursors are specified by HH10, concomitant with their complete segregation from other placodal, epidermal and neural progenitors. Heterotopic transplantation of olfactory progenitors reveals they are capable of autonomous differentiation only 12 hours later, shortly before overt placode invagination at HH14. Taken together, these results show that olfactory placode development is a step-wise process whereby signals from adjacent tissues specify competent ectoderm at or before HH10, followed by gradual commitment just prior to morphological differentiation.

KEY WORDS: Olfactory placode, Nasal placode, Chick, Competence, Specification, Commitment, Induction, Ectoderm

INTRODUCTION

Cranial sensory placodes arise as transient thickenings of embryonic head ectoderm (van Wijhe, 1883; von Kupffer, 1891) and invaginate/ingress to form components of the nose, lens and inner ear (Bailey and Streit, 2006; Baker and Bronner-Fraser, 2001; Schlosser, 2006). Of the three sensory placodes, the lens and otic are relatively easy to distinguish and manipulate early in development. Therefore, tissue interactions and signals guiding their induction have been studied extensively (reviewed by Brown et al., 2003; Chow and Lang, 2001; Donner et al., 2006; Grainger, 1992; Noramly and Grainger, 2002; Riley and Phillips, 2003; Saha et al., 1989; Streit, 2001; Torres and Giraldez, 1998).

By contrast, development of the olfactory sensory system has been primarily investigated at later stages. An attractive model for studying neurogenesis, its myriad of derivatives include the regenerative odorant sensing olfactory neurons in the olfactory epithelium (Calof et al., 1998; Graziadei and Graziadei, 1979; Graziadei and Metcalf, 1971; Graziadei and Monti Graziadei, 1983), the ingressing gonadotropin-releasing hormone neurons (reviewed by Parhar, 2002; Wray, 2002) [for a contrary view see Whitlock (Whitlock, 2005)], the pheromone-detecting vomeronasal organ (Dulac, 1997) and other neuromodulatory and neuroendocrine cells (Northcutt and Muske, 1994; Tarozzo et al., 1995; Yamamoto et al., 1996). It is the only placode to give rise to glial cells that ingress and migrate along the olfactory nerve towards the brain (Chuah and West, 2002; Ramon-Cueto and Avila, 1998). Cues that guide differentiation along these different pathways and the molecular mechanisms underlying the patterned wiring of olfactory sensory neurons have been examined extensively (reviewed by Baker and Margolis, 2002; Balmer and LaMantia, 2005).

Contrasting with this wealth of data, inductive events that initiate olfactory development remain ambiguous, partially because the placode is morphologically invisible until relatively late (HH13+ in birds). Transplantation studies show that precursors straddle the lateral anterior neural folds and adjacent ectoderm in the neurula (Couly and Le Douarin, 1985), but their exact location at intervening stages was unclear. Recent cell marking studies in zebrafish and chick have examined the origin of the olfactory placode at higher resolution and at intervening stages (Bhattacharyya et al., 2004; Whitlock and Westerfield, 2000). Olfactory precursors are initially distributed in a broad region spanning the anterior neural folds and overlapping with lens precursors. Over time, they become progressively restricted to the most anterior ectoderm, finally resolving to a discrete olfactory pit. Knowledge of the location of precursors at different stages has facilitated manipulation of their development.

To understand how and when the nasal epithelium is first induced, we examined competence, specification and commitment of ectoderm toward an olfactory fate. This information is a necessary prerequisite for interpreting results of functional perturbations at the molecular level. First, we correlated molecular markers with a more complete fate-map (Bhattacharyya et al., 2004) and found that *Dlx3*, *Dlx5* and *Pax6* can serve as molecular guideposts for olfactory placode precursors at different stages. Although an initially broad region of head ectoderm is competent to form olfactory placode, this ability is restricted with time. In vitro explant assays suggest that placode induction by adjacent tissues occurs by ~HH10, when olfactory precursors have segregated from their neighbors. In vivo heterotopic transplantation studies demonstrate that commitment occurs with a time lag of 12 hours. This suggests a period of developmental plasticity, perhaps accounting for the regulative nature of early olfactory placode development. This step-wise progression of placode formation favors flexibility in fate until such time as the placode becomes morphologically apparent.

MATERIALS AND METHODS

Quail-chick grafts

Fertilized chick and quail eggs were incubated at 38°C to the desired stage (Hamburger and Hamilton, 1951). Host embryos were visualized using India Ink or dye, and the vitelline membrane removed. Before HH8, clean quail ectoderm was obtained without enzymatic treatment. Between HH10-16, donor ectoderm was separated from mesenchyme and forebrain using 1 mg/ml dispase+0.25% trypsin in DMEM (Boehringer Mannheim;

Division of Biology, 139-74, California Institute of Technology, Pasadena, CA 91125, USA

*Author for correspondence (e-mail: mbronner@caltech.edu)

Accepted 17 October 2008

30 minutes on ice, 10 minutes at 37°C) or +0.2–0.25% collagenase (Worthington) in PBS (20 minutes at 37°C). Mid/hindbrain level ectoderm was dissected from neural crest using 1 mg/ml dispase. Ectoderm pieces were washed and allowed to recover before grafting and positioned in the correct inside-outside orientation; embryos were incubated for 48-72 hours and fixed in 4% paraformaldehyde. Seventy out of 264 surviving chimaeras showed appropriate graft incorporation.

Collagen gel cultures

Quail embryos (HH8,10,14) were collected in Ringer's solution. Small pieces of HH8 anterior ectoderm or HH10-14 presumptive olfactory placode were dissected as above and stored in PB1 medium on ice until use. Collagen (90 μl; Collaborative Research) +10 μl of 10× DMEM (Invitrogen) in 0.375% sodium bicarbonate was solidified in four-well plates (Nunc); tissue pieces were transferred, overlaid with 5 μl collagen mix, immersed in 0.5 ml of the defined medium, F12+N2 (Invitrogen), incubated for 24-48 hours at 37°C with 5% CO_2, then fixed in 4% paraformaldehyde for 30 minutes at room temperature.

Electroporation of HH10 ventral ectoderm

pCIG-GFP plasmid DNA (Megason and McMahon, 2002) was injected at a concentration of 2.5 μg/μl in Ringer's solution with 50 ng/μl Fast Green between the embryo's ventrum and extra-embryonic ectoderm at HH10-11. Platinum electrodes (4 cm long and 4 mm apart) and the electroporator were custom-built in our laboratory and by the electronics shop, respectively. The positive electrode was placed on top and the negative electrode under the anterior tip of the embryo and five pulses of 8-10V for 50 ms at 100 ms intervals were applied. Embryos were reincubated until HH18 or 27 (23/47 and 14/29 survivors, respectively), collected, fixed in 4% paraformaldehyde overnight at 4°C and prepared for cryosectioning.

Histology, immunocytochemistry and imaging

Embryos and collagen gels were embedded in 7.5% gelatin in 15% sucrose and cryosectioned. Sections were degelatinized, stained with antibodies in blocking solution, rinsed and mounted in Fluoromount-G (Southern Biotechnology) or Permount containing 10 μg/ml DAPI. Primary antibodies were: QCPN (DSHB; 1:1), QCPN conjugated to Alexa-568 (at the University of Oregon; 1:50), Pax6 rabbit polyclonal (Covance; 1:100), Pax7 monoclonal (DSHB; 1:20), Dlx3 goat polyclonal (1:1500), pan-Dlx rabbit polyclonal (Dr Jhumku Kohtz; 1:70), Hu monoclonal (Molecular Probes; 1:250), chick GnRH-I rabbit polyclonal (Dr James Millam; 1:100) and mouse GnRH-I rabbit polyclonal (Abcam; 1:100). Antibodies against the mouse and chick GnRH-I peptides, which differ at amino acid position 8, were used concurrently to maximize staining efficiency. Secondary antibodies used include Molecular Probes Alexa 488 and Alexa 568 (1:1000-1:2000), and Jackson ImmunoResearch AMCA and Cy5 (1:200-1:400).

Tri-color images were acquired on a Zeiss Axioskop2 using an Axiocam Mrm camera and Axiovision software or a Zeiss LSM 510 Meta confocal microscope.

Antibody generation and immunoblot analysis

GST-C-terminal chick Dlx3 fusion protein (amino acids 185-278) was produced in BL-21 cells and purified using Glutathione Sepharose beads (Pharmacia) (Sambrook and Russell, 2001). Goats were injected with 5 mg Dlx3 protein (Alpha Diagnostic). Immunoblots and immunostaining confirmed specificity of each bleed.

Whole-mount in situ hybridization

Whole-mount in situ hybridization was performed as described (Streit and Stern, 2001) at a hybridization temperature of 70°C using cDNAs for Dlx3 (Dr Andy Groves), Pax6 and Dlx5 (Dr Michael Kessel).

RESULTS

Multiple homeodomain transcription factors are expressed in the forming olfactory placode

Avian olfactory placode development was followed from dispersed cells in the ectoderm to the morphologically thickened and invaginated olfactory pit, taking advantage of the spatiotemporal expression of several transcription factors that cumulatively reflect acquisition of olfactory fate. Chick Dlx5 and Pax6 transcripts are detected as early as HH6 (neurula stage) in olfactory and lens precursors in anterior cranial ectoderm (Bhattacharyya et al., 2004). Their overlap is maintained until just before HH10, when Dlx5 is upregulated and Pax6 is simultaneously downregulated in presumptive olfactory placode cells (Fig. 1B,C,E,F) (Bailey et al., 2006). At HH8, both Pax6 and Dlx5 are expressed in a 'salt and pepper' pattern in ectoderm abutting the neural folds containing nasal precursors (Fig. 1B,B″,C,C′) (Bhattacharyya et al., 2004); anterior-most ectoderm expresses Dlx5 uniformly (Fig. 1B′). Pax6 expression is also observed within anterior neural folds, which contribute to olfactory epithelium and telencephalon (Fig. 1C). Conversely, Dlx3 is absent from anterior neural folds and low in adjacent ectoderm at HH8 (Fig. 1A,A′), but strongly upregulated in olfactory placode precursors at HH10 (Fig. 1D,D′) (Pera and Kessel, 1999). Expression refines over time to the medioventral region of the head ectoderm between the forming eyes (Fig. 1G,G′). By HH11, olfactory precursors occupy a discrete region in the ventral ectoderm (Bhattacharyya et al., 2004), where Dlx5 is expressed continuously (Fig. 1E,E′), but Pax6 is extinguished (Fig. 1F,F′). Interestingly, Pax6 is re-expressed once the olfactory placode has formed at HH14 (Fig. 1I,I′), contiguous to corneal Pax6 expression (Fig. 1I′, arrow) and subsequently spreads anteromedially. The thickened placode shows continued expression of Dlx3 and Dlx5 transcripts at HH14+ (data not shown) (Fig. 1H,H′). The first co-expression of all three transcripts is coincident with morphological appearance of the olfactory placode.

As expected, no marker gene is expressed exclusively in the mature olfactory placode/pit by HH19-20 (Fig. 2A-C′). While Dlx3 is found in olfactory and otic placodes (Fig. 2A,A′), Dlx5 is also expressed in the adenohypophysis and both are expressed in subpopulations of neural crest (Fig. 2A,B; data not shown). Dlx3 is expressed in cranial crest populating distal elements of branchial arches 1-2 (Fig. 2A) (Depew et al., 2005; Pera and Kessel, 1999), whereas Dlx5 is more widely expressed in branchial arches 1-4 and the trigeminal ganglion (Fig. 1H,H′; Fig. 2B) (Pera et al., 1999). Dlx5 is also evident in newly emergent trunk neural crest (Fig. 3B). Like the Dlx genes, Pax6 is expressed at multiple sites, including lens and nasal placodes (Fig. 2C,C′). However, combined expression of Pax6 and Dlx genes by HH19 is unique to the olfactory placode.

Unlike Dlx3 and Pax6, Dlx5 is expressed in a few cells in the mesenchyme as the olfactory placode thickens (Fig. 1H′, arrow), even continuing to HH20 (Fig. 2B′, arrowhead). This raises the intriguing possibility that it marks a subset of neuronal cells ingressing from the olfactory placode. To test this, HH10 ventral ectoderm was electroporated with a GFP construct (survivors n=37) and examined for expression of Dlx and GnRH neuropeptide. At HH18, GFP+ cells are Dlx+ within the olfactory epithelium (Fig. 2D,d). Moreover, ingressing GFP+/Hu+ neurons are also Dlx+ (Fig. 2d′,d″). At HH27, by which time GnRH neurons are detectable (Fig. 2G) (Mulrenin et al., 1999), some GnRH+/GFP+ cells were located within a ganglion-like structure between the epidermis and ventral forebrain (Fig. 2e,f), unequivocally demonstrating their placodal rather than neural crest origin. Adjacent sections also had GFP+/Dlx+ cells (Fig. 2e′,f′), leading to the conjecture that some GnRH cells may co-express Dlx; direct double-labeling was not possible as both antibodies were raised in the same species.

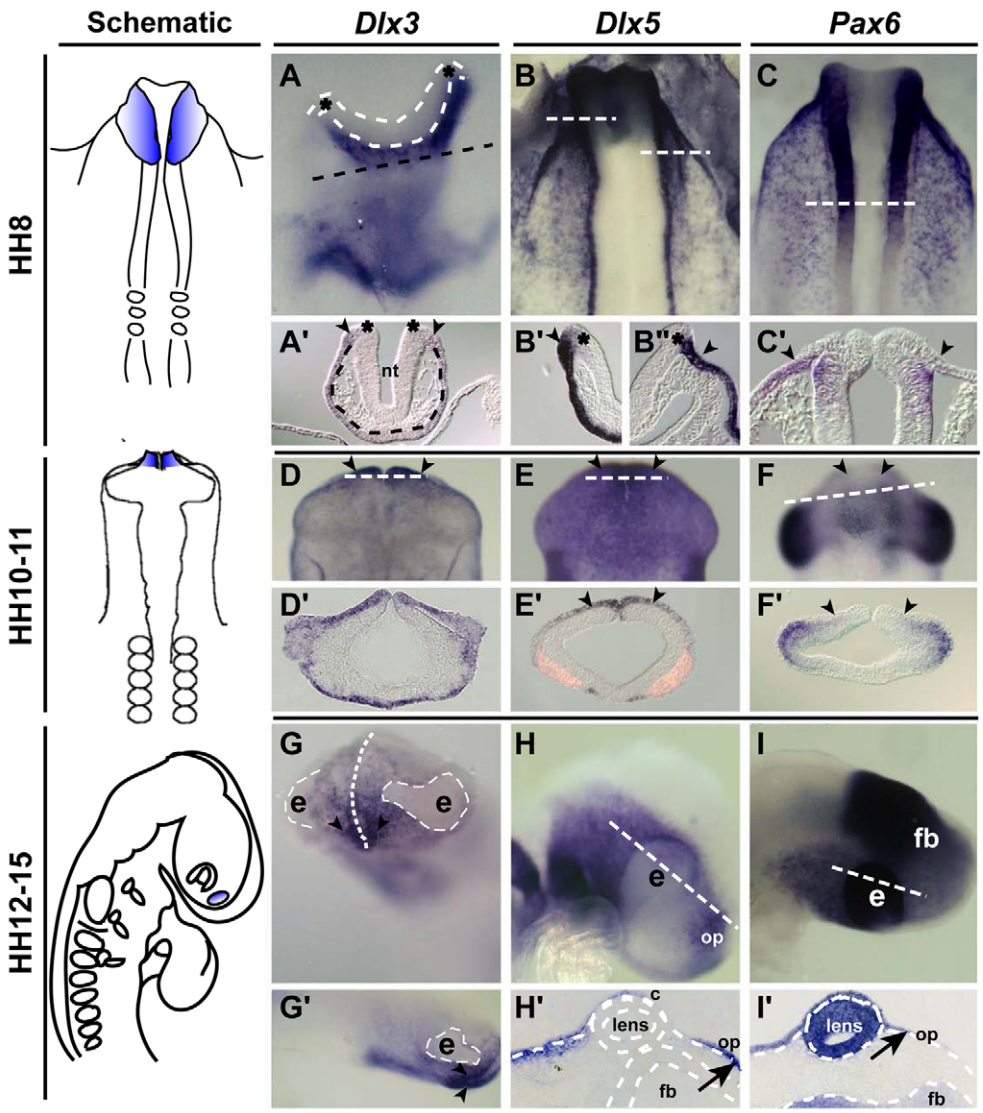

Fig. 1. Expression of *Dlx3, Dlx5* and *Pax6* in chick olfactory placode precursors. (A,A′,D,D′,G,G′) *Dlx3*. (B-B″,E,E′,H,H′) *Dlx5*. (C,C′,F,F′,I,I′) *Pax6*. (**A**,**A′**) Ventral view of *Dlx3* at HH8. Broken white lines trace outline of anterior neural fold region. Asterisks indicate olfactory precursor regions lacking Dlx3 expression in A and A′. Broken black line in A indicates transverse plane of section shown in A′. Low-level expression is seen in ectoderm adjacent to anterior neural folds (A′, arrowheads). Broken line in A′ outlines ectoderm. (**D**,**D′**) Ventral view and transverse section, respectively, of *Dlx3* at HH10 show strong expression in olfactory progenitors (arrowheads). (**G**) At HH13, *Dlx3* refines ventromedially (arrowheads) within anterior ectoderm between eyes (outlined); midline of embryo denoted by a single white dotted line. (**G′**) Lateral view of embryo shown in G. The eye is outlined and arrowheads indicate *Dlx3* expression in nasal progenitors. (B) Dorsal view of *Dlx5* at HH8. (**B-B″**) Low transcript levels within anterior neural folds (asterisks) with gradual posterior decline and exclusion from posterior neural folds (compare B′ with B″). *Dlx5* is expressed at high levels within the anterior ectoderm, but shows 'salt and pepper' expression more posteriorly (compare B′ with B″). Arrowheads indicate *Dlx5* expression in adjacent ectoderm. (**E**,**E′**) Ventral view and transverse section, respectively, of *Dlx5* at HH11. Arrowheads indicate strong expression in olfactory precursors. HNK-1 staining in pink in E′ shows distance of neural crest from placode precursors at this stage. (**H**,**H′**) *Dlx5* at HH15 is in migrating neural crest and olfactory placodes (arrow in H′ section indicates *Dlx5*+ thickened ectoderm or ingressing placode cells). (C,C′,F,F′,I,I′) *Pax6* at HH8 (C, dorsal view; C′, section), HH11 (F, ventral view; F′, section) and HH14 (I, lateral view; I′, section). (**C**,**C′**) Abundant *Pax6* in anterior neural folds and salt-and-peppered throughout anterior ectoderm (arrowheads in C′). (**F**,**F′**) High levels in eye, but extinguished in olfactory precursors (between arrowheads, F,F′). (**I**) Robust *Pax6* in eye and diencephalon at HH14. (**I′**) Arrow indicates reappearance of *Pax6* in presumptive nasal ectoderm. Broken white lines indicate planes of section in B-F,H,I. c, cornea; nt, neural tube; e, eye; fb, forebrain; op, olfactory placode. The schematic drawings on the left show the position of the olfactory precursors (blue) at the indicated stages.

Dlx3-specific polyclonal antibody reveals Dlx3 protein distribution

To detail temporal expression of Dlx3 protein in the developing olfactory placode, we generated a polyclonal antibody against the C terminus of chick Dlx3, a region of minimal similarity between the six Dlx family members. The polyclonal antibody recapitulates Dlx3 mRNA expression, though the protein has more widespread expression in ectoderm than the mRNA (compare Fig. 2A′ with Fig. 3C). To ensure against crossreactivity with Dlx5, which has highest sequence homology and maximum expression overlap, we compared localization of Dlx5 and Dlx3 transcripts and protein. At HH11, the otic placode at the rhombomere (r) 5 level begins to express Dlx5 weakly (Fig. 3A), while strongly expressing Dlx3 (not shown). HNK1+ neural crest cells atop the neural tube, however, express Dlx5 robustly (compare outlined domains in Fig. 3A,A′). The Dlx3 antibody clearly recognizes otic placode cells (also HNK1+) but not dorsal neural tube, conclusively demonstrating lack of crossreactivity with Dlx5 (compare Fig. 3A and Fig. 3A′). Similarly, emigrating trunk neural crest expresses Dlx5 but not Dlx3 (compare Fig. 3B with Fig. 3B′). To ensure against crossreactivity with other Dlx family members, we co-labeled sections through heads of 3-day-old chick embryos with Dlx3 and pan-Dlx antibodies (Panganiban et al., 1995). Dlx3 is the only family member not expressed in the CNS for the first three days (data not shown) (Beanan and Sargent, 2000; Liu et al., 1997; Panganiban and Rubenstein, 2002; Pera and Kessel, 1999; Price, 1993; Robinson and Mahon, 1994) (see also Dhawan et al., 1997; Zhu and Bendall, 2006). However, it is expressed robustly in the olfactory epithelium at HH18-19 (Fig. 3C). Other Dlx family members expressed in the olfactory epithelium include Dlx5/6 (Brown et al., 2005; Pera and

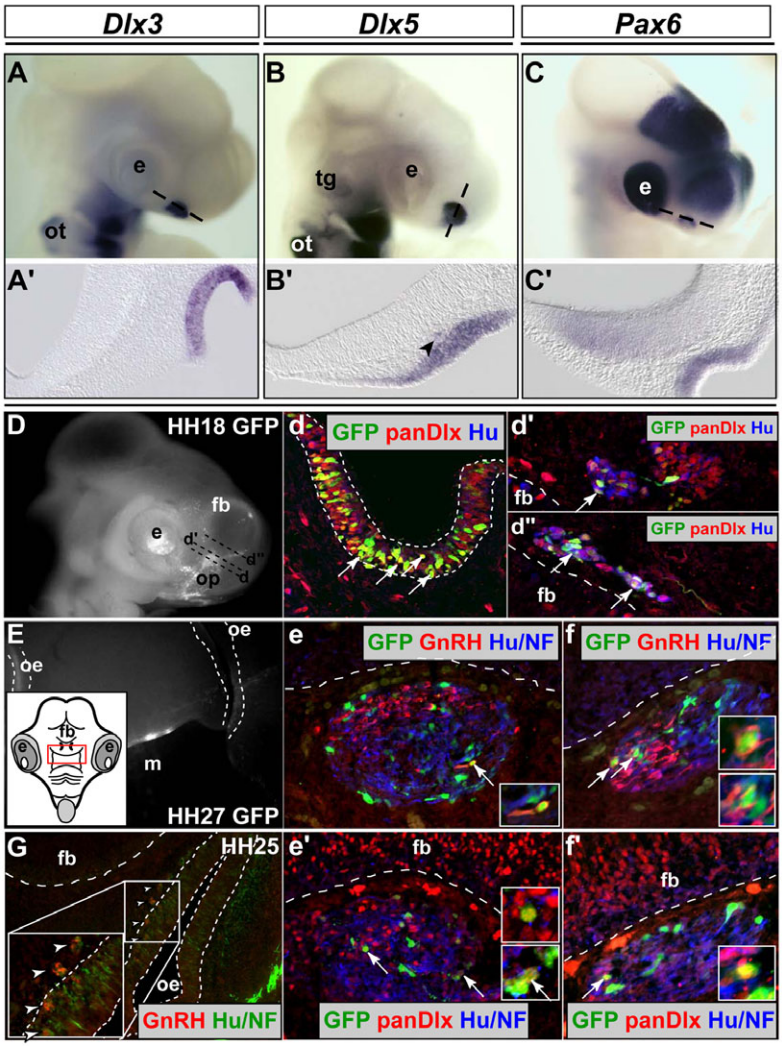

Fig. 2. Dlx+ and GnRH+ neurons found in the nasal mesenchyme have a placodal origin. (**A-C′**) *Dlx3, Dlx5* and *Pax6* in olfactory epithelium at HH19-20. Levels of *Dlx3* are strong throughout the olfactory pit (A,A′) and also in the otic pit (ot) and branchial arches. (B) *Dlx5* is expressed in olfactory and otic placodes, broadly in branchial arches, in the neural crest-derived part of trigeminal ganglion (tg) and in ingressing olfactory placode cells (B′, arrowhead). (C) *Pax6* is expressed in olfactory pit, eye (e) and forebrain. (C′) Section through olfactory placode. Broken black lines indicate planes of section. (**D-f′**) Placodal origin of GnRH neurons. (D) Whole-mount view of HH18 embryo electroporated with pCIG-GFP at HH10. Broken black lines indicate transverse sections through the olfactory epithelium shown in d-d″. (d) Section through the olfactory pit. Arrows indicate multiple GFP+(green)/pan-Dlx+(red) cells. (d′,d″) Sections through more basal regions of the olfactory system. Neurons (indicated by arrows, Hu+, blue) that ingress from the placode (GFP+,green) are also Dlx+. (E) Ventral whole-mount view of HH27 embryo electroporated with pCIG-GFP at HH10; inset shows schematic of ventral view of HH27 embryo, red box indicates area shown at high magnification. (e) Numerous GFP+ (green) cells are observed in a ganglion-like structure. Arrow indicates a GFP+ GnRH neuron (inset). (e′) A nearby section has pan-Dlx+/GFP+ cells (arrows; insets). (f,f′) Sections through a similar embryo. Arrows indicate GFP+/GnRH+ neurons (f) and GFP+/pan-Dlx+ neurons in an adjacent section (f′). Higher magnification views can be seen in insets. (**G**) Transverse section through the olfactory epithelium of a non-electroporated HH25 chick embryo. GnRH (red) Hu/neurofilament (green)-positive neurons (indicated by arrowheads) are seen within the olfactory epithelium and just ventral to it. oe, olfactory epithelium; m, maxillary epithelium; fb, forebrain; e, eye.

Kessel, 1999). The pan-Dlx antibody recognizes all chick Dlx proteins; therefore, strong co-localization of both the Dlx3 and pan-Dlx antibodies is noted in the nasal pit (Fig. 3C′; Fig. 3C″, yellow). Dlx1, 2, 5 and 6 are expressed in the telencephalon at various times in many vertebrates, including chick (Eisenstat et al., 1999; Liu et al., 1997; Panganiban and Rubenstein, 2002), and are detected by the pan-Dlx but not the Dlx3-specific antibody (Fig. 3C″). These data indicate that the chick Dlx3 antibody is specific and does not crossreact with closely related family members.

Co-expression of Dlx3 and Pax6 proteins correlates with acquisition of olfactory fate

We next investigated colocalization of Dlx3 and Pax6 in cells fated to form olfactory placode at single cell resolution. Just prior to olfactory placode thickening (HH13), Dlx3 protein is present at high levels in forebrain-level ectoderm (Fig. 3D,D″), whereas Pax6 protein is in scattered cells more laterally (Fig. 3D′,D″). The number of cells co-expressing both progressively increases such that by HH19-21, robust expression of Dlx3 and Pax6 proteins is noticeable in the now pseudostratified placode epithelium (Fig. 3E-E″). Significant overlap is seen in the cup-shaped olfactory epithelium (Fig. 3E″) though domains of solely Dlx3+ or Pax6+ cells are also observed. Similar results were seen in quail embryos (data not shown).

The first signs of differentiation occur at ~HH14, when earliest ingressing placode cells express the RNA-binding protein Hu, which marks post-mitotic neurons (Fornaro et al., 2001; Fornaro et al., 2003). By pit stages, Hu labels abundant neurons within the epithelium, which express Pax6 and/or Dlx3, as well as those migrating along the olfactory nerve towards the telencephalon (Fig. 3F,G). Ultimately, Pax6 expression is only maintained in a subpopulation of non-neuronal cells in the nascent olfactory epithelium (Davis and Reed, 1996). Dlx3+ neurons are unique to the olfactory system at least at HH19, although Dlx3 expression has been reported in the ventral forebrain at HH27-29 (Zhu and Bendall, 2006). Accordingly, we observed Dlx3+ but Hu– cells in the midline between the two telencephalic vesicles at HH19 (not shown).

Interactions between placodal ectoderm and frontonasal mesenchyme, which is largely neural crest derived (Osumi-Yamashita et al., 1994; Serbedzija et al., 1992), play a pivotal role in orchestrating development and differentiation of the nasal epithelium and capsule (Bailey et al., 2006; Firnberg and Neubüser, 2002; LaMantia et al., 2000). To assess the contribution of neural crest cells to olfactory placode specification and commitment, we used Pax7 as a marker for neural crest and the lateral domain of frontonasal mesenchyme (Fig. 3H) (Firnberg and Neubüser, 2002).

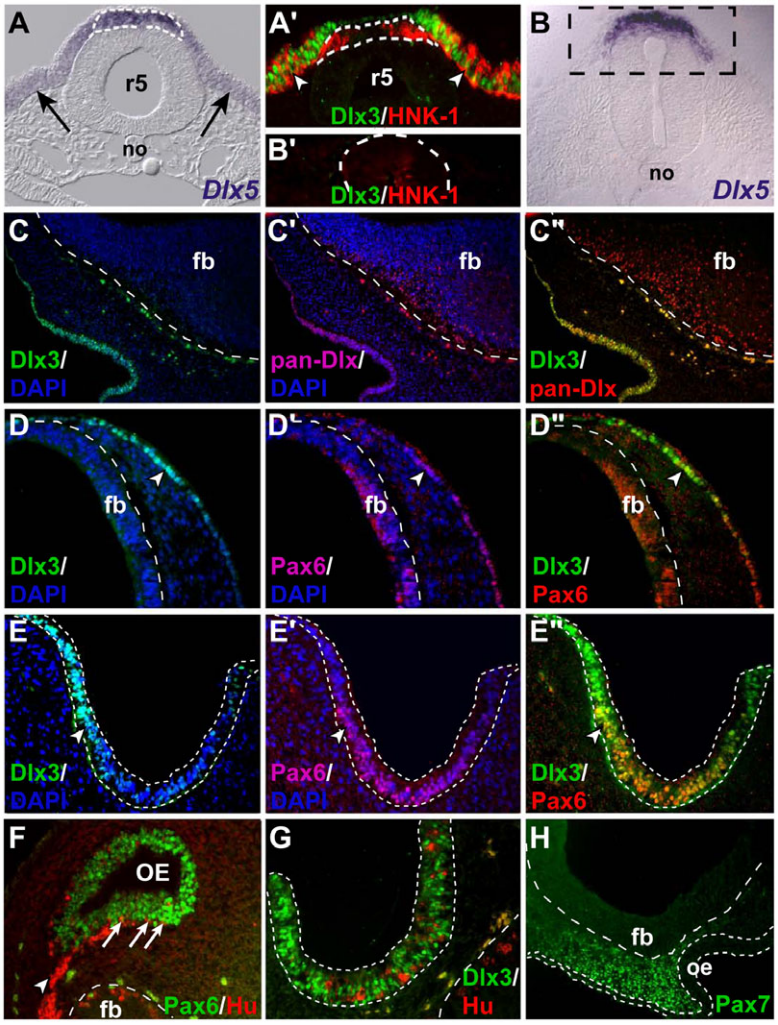

Fig. 3. Dlx3 protein co-expresses with other Dlx family members, Pax6 and Hu in the olfactory epithelium. (**A-C″**) Specificity of Dlx3 antibody. (A) Section through r5 at HH11. Premigratory neural crest prominently expresses *Dlx5* (broken white lines). Lower levels are also detected in otic placode (arrows). (A′) HNK1+/Dlx3+/Dlx5+ (from A) otic placode (white arrowheads) and HNK+/Dlx5+ (from A) but Dlx3– (green) neural crest (white dotted lines). (B) In the trunk, Dlx5 transcripts are abundant in dorsal neural tube and emigrating neural crest. (B′) No Dlx3 or HNK1 staining is noted in dorsal neural tube or neural crest. (C-C″) Cryosections of HH19-20 embryos co-stained for Dlx3 (green), pan-Dlx (red) and DAPI (blue) show overlap between two antibodies (C″, yellow) in olfactory, but not in forebrain, which lacks Dlx3, but stains with pan-Dlx (red). (**D-D″**) Dlx3 and Pax6 protein in forming olfactory placode (white arrowheads) at HH14. (D) Dlx3 (green) is in ectoderm proximal to forebrain (fb). (D′) Pax6 (red) is in scattered cells but stronger in posterior ectoderm of future cornea. (D″) Overlay of Dlx3 and Pax6 shows some co-expression (yellow; D-D″, arrowheads). (**E-E″**) Dlx3 and Pax6 protein in olfactory epithelium at HH20. (E) Dlx3 (green) is found throughout the epithelium, but higher at margins. (E′) Pax6 (red) is in cup-shaped olfactory epithelium. (E″) Dlx3 and Pax6 are co-expressed in many cells (yellow; E-E″, arrowheads). DAPI is in blue in D-E″. (**F**) By HH19, olfactory epithelium undergoes robust neurogenesis (pan-neuronal Hu is in red) and ingressing neurons are observed (arrowhead); some neurons within the epithelium are Pax6+ (green, arrows). (**G**) At HH21, a few neurons are also Dlx3+. (**H**) Nasal mesenchyme underlying olfactory pit at HH18-19 is Pax7+ (green). fb, forebrain; oe, olfactory epithelium; no, notochord.

Epiblast is competent to form olfactory placode

Fate maps (Couly et al., 1985; Bhattacharyya et al., 2004) suggest that the chick nasal placode arises from around the anterior neural folds at HH8. Accordingly, isotopic and isochronic quail/chick grafts of HH8 anterior neural fold (Fig. 4a) or adjacent ectoderm (Fig. 4b) gave rise to quail cells [distinguished using quail cell peri-nuclear (QCPN) antigen] in the olfactory placode 2-3 days later (Fig. 4A′,B′). Donor cells expressed Dlx3, Pax3 (data not shown), Pax6 (n=6) (Fig. 4A-A″,B-B″) and differentiated as neurons. Because olfactory precursors closely associate with both lens and forebrain progenitors (Bhattacharyya et al., 2004), quail cells were additionally found in the telencephalon (Fig. 4A′, arrow; Fig. 4A″) or ectoderm adjacent to the olfactory placode including parts of the cornea and lens (Fig. 4B′; data not shown).

To determine the earliest time when ectodermal precursors are capable of responding to olfactory placode-inducing cues, HH4-5 (gastrula to early neurula) anterior or lateral epiblast (adjacent to the area opaca) was heterochronically grafted into ectoderm adjacent to the anterior neural fold at HH8. This most anterior or lateral epiblast does not contribute to neural ectoderm but eventually forms non-neural ectoderm, neural crest and otic placode (Fernandez-Garre et al., 2002; Garcia-Martinez et al., 1993; Rosenquist, 1966; Schoenwolf and Alvarez, 1991), none of which co-express Pax6/Dlx3 and form Dlx3+ neurons. However, this epiblast can express Pax6 and Dlx3 in the olfactory placode when grafted to anterior neural fold region (n=3) (Fig. 4c,C-C″; data not shown). Interestingly, grafted tissue underwent thickening and invagination to form another placode-like structure when incorporated aside the endogenous olfactory placode (Fig. 4C′, boxed area). A few graft-derived cells differentiated into Dlx3+ olfactory neurons in the thickened epithelium (compare Fig. 4C″ and Fig. 4D″). Additionally, we noted many quail Hu+ cells lining the olfactory nerve (Fig. 4D″, inset). This demonstrates that though epiblast tissue is regionally specified (Wilson et al., 2001), it nonetheless is plastic and retains competence to respond to diverse inducing signals and differentiate accordingly.

Competence to form olfactory placode is restricted to head ectoderm

We determined the competence of ectoderm at different axial levels to contribute to olfactory epithelium and express olfactory markers as a function of time by grafting surface ectoderm from HH8-13 donor quails, to the prospective nasal territory of HH7-9 chick hosts. Chimaeras were allowed to survive until the olfactory pits were distinctly visible (HH18: ~48-72 hours later).

Midbrain-level ectoderm

Midbrain-level ectoderm, which is fated to contribute to trigeminal ganglion (D'Amico-Martel and Noden, 1983; Xu et al., 2008), robustly expresses Pax3 from HH8 (Stark et al., 1997), as well as low

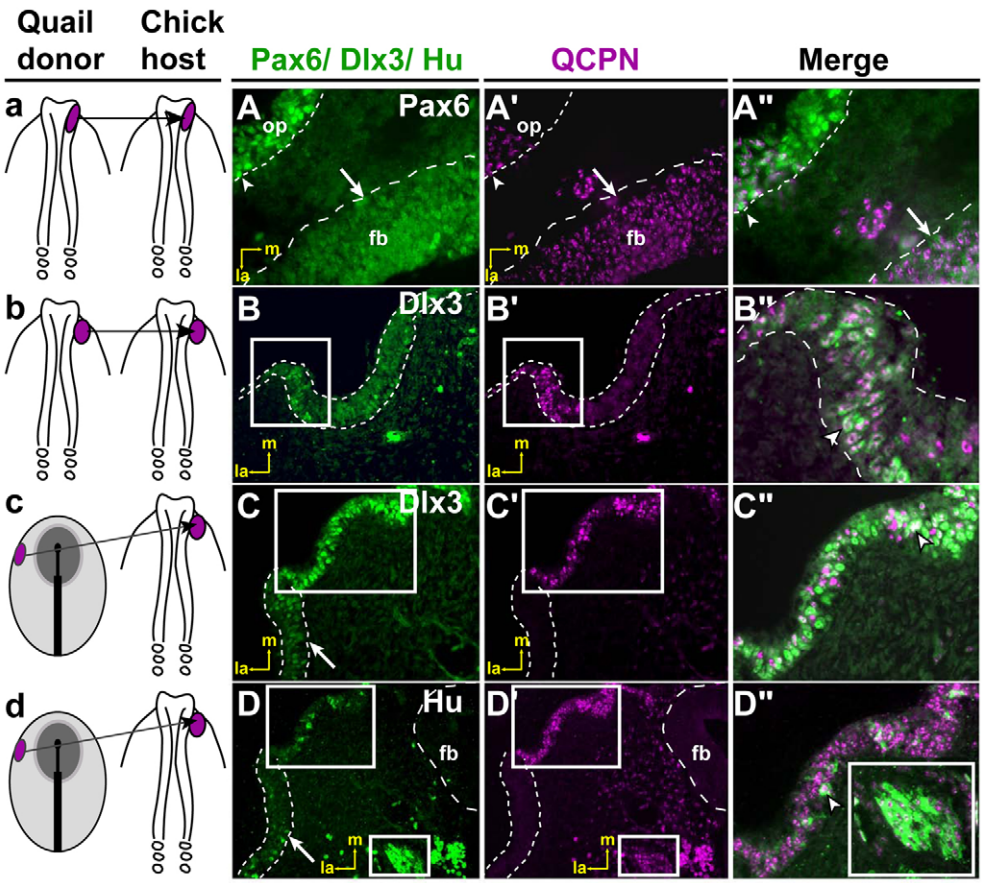

Fig. 4. Isotopic/isochronic grafts and naïve epiblast grafts to presumptive olfactory placode ectoderm contribute to endogenous olfactory epithelium. (**a-A″**) After grafting anterior neural folds from HH8 quail, Pax6+ quail cells are in olfactory epithelium (A-A″, arrowheads) and telencephalon (A-A″, arrows). (**b-B″**) HH8 ectoderm grafted adjacent to anterior neural folds contributes to nasal pit and adjacent ectoderm (boxes in B,B′, arrowhead indicates Dlx3+/QPCN+ cell). (**c-D″**) HH5 quail epiblast grafted to presumptive olfactory territory integrated into ectoderm adjacent to placode, thickened and expressed Dlx3 (box in C,C′; arrow indicates Dlx3+ host nasal pit; arrowhead indicates Dlx3+/QCPN+ cell). Hu staining (D-D″) shows extensive neuronal differentiation. In D,D′, large box indicates neurons in grafted epithelium and small box indicates quail cells contributing to the olfactory nerve. Arrowhead indicates Hu+/QCPN+ cell (D″). Inset in D″ shows high magnification of neurons migrating from donor-derived olfactory placode. la, lateral; m, medial; op, olfactory placode; fb, forebrain.

levels of Pax6 at HH8 (Fig. 1C) and Dlx3 at HH10 (not shown). However, their expression is not maintained in the ophthalmic trigeminal (opV) placode (Fig. 2A,C). Therefore, we looked for prolonged expression of these markers and concomitant neurogenesis in midbrain level ectoderm grafted adjacent to anterior neural folds (Fig. 5b,c) (*n*=15). HH8 presumptive opV placode ectoderm expresses both Dlx3 and Pax6 at high levels following incorporation into the olfactory placode and robust expression is maintained in grafted ectoderm taken from HH10 embryos (Fig. 5B-B″). Similarly, opV placode ectoderm that simultaneously incorporates into cornea and lens, expresses high levels of Pax6 in these novel locations (Fig. 5E,F). Additionally, quail neurons contribute to the migratory mass lining the olfactory nerve (Fig. 5C-C″). Shortly after HH10, Pax6 expression is extinguished in grafted cells. In fact, ectoderm grafts taken from HH12 and onwards show no Pax6 expression in peripheral ectoderm that is ordinarily Pax6+. Weak expression is observed in a few cells only if the graft incorporates into the placode (data not shown).

Hindbrain-level ectoderm

Ectoderm adjacent to r1-6, including presumptive otic placode ectoderm (Couly and Le Douarin, 1990; Groves and Bronner-Fraser, 2000; Streit, 2002) was tested for its potential to contribute to olfactory placode (*n*=16). Hindbrain-level ectoderm does not express Pax6 at early stages in situ; however, Dlx3 is expressed at high levels by otic ectoderm from HH9 onwards and at low levels in ectoderm rostral to otic ectoderm (Pera and Kessel, 1999) (data not shown). Hindbrain-level ectoderm (HH8–) can replace ablated nasal progenitors and express both Dlx3 (Fig. 5A-A″) and Pax6 plus generate placode-derived neurons that line the olfactory nerve. Shortly thereafter, Pax6 expression is no longer induced in hindbrain-level ectoderm, even when it spans the corneal ectoderm, which usually expresses Pax6 at high levels (Fig. 5G). However, three cells that contribute to the lens express Pax6 at this stage (HH8+) (Fig. 5G, arrowhead). Dlx3 is only weakly induced at these stages (data not shown). Neither gene is expressed in grafts of pre-otic ectoderm from HH10-11 embryos; instead, otic-derived ectoderm expresses Pax2 (an otic placode marker) in its new location. Thus, hindbrain-level ectoderm loses capacity to respond to olfactory placode-inducing signals with age more rapidly than midbrain level ectoderm.

Trunk level ectoderm

Trunk level ectoderm does not express Dlx3 except in the flank that forms the apical ectodermal ridge of the limbs. It never expresses Pax6 nor gives rise to placodes. To test for placodal competence, trunk level ectoderm (*n*=5) at the level of the 5th-9th somites was heterotopically transplanted adjacent to the anterior neural folds of HH8 to HH8+ embryos. Although the grafted ectoderm could not express Pax6 even at the earliest ages tested (HH8–) (Fig. 5D-D″), it could express Dlx3 up until HH9–. Thus, competence to express olfactory markers was particularly short-lived in trunk ectoderm.

In conclusion, all levels of head ectoderm (which have some degree of placodal bias) are competent to form Dlx3+/Pax6+ cells and Hu+ neurons in olfactory epithelium and along the olfactory nerve. However, the level of competence in embryonic ectoderm is graded such that ectoderm closest to olfactory progenitors remains competent for the longest duration.

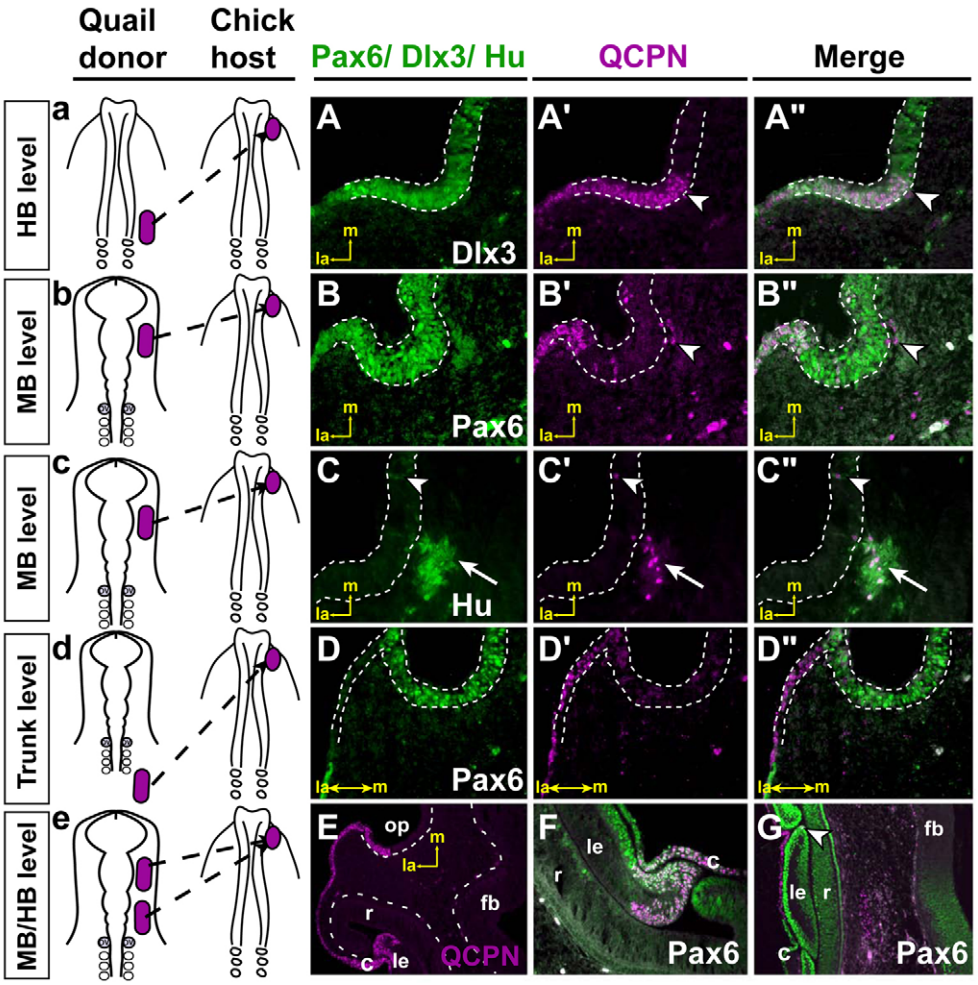

Fig. 5. Head but not trunk ectoderm is competent to form olfactory placode. (**a**) HH8 hindbrain-level ectoderm expresses Dlx3 when grafted to presumptive nasal region (**A-A″**; arrowhead points to a Dlx3+/QCPN+ cell). (**b**) HH10 midbrain-level ectoderm expresses Pax6 when grafted to olfactory placode region (**B-B″**; arrowhead indicates an ingressing QCPN+ cell). (**c-C″**) Similar graft to b undergoes neuronal differentiation within olfactory pit (C-C″, arrowheads) and in ingressing cells lining olfactory nerve (C-C″, arrows). (**d-D″**) Grafts of HH8 trunk-level ectoderm fail to express Pax6. (**e**,**E**) Some head ectoderm grafts incorporate into nose, lens and cornea. (**F**) HH8 midbrain-level ectoderm expresses Pax6 in lens and cornea. (**G**) HH8+ hindbrain-level ectoderm is not competent to express Pax6 in cornea or olfactory placode (not shown), though three quail cells in the lens appear Pax6+ (arrowhead). la, lateral; m, medial; c, cornea; fb, forebrain; le, lens; op, olfactory placode; r, retina.

Nasal placode precursors are specified toward olfactory fate by HH10, prior to acquiring placodal morphology

Classically, specification is defined as the potential of tissue explanted and grown without additional activating/inhibitory differentiation signals, indicating their degree of progression along a particular developmental pathway. To determine the time by which olfactory induction had occurred, presumptive olfactory ectoderm was cultured without serum for 24-72 hours in three-dimensional collagen gels. Expression of Pax6, Dlx3 and neuron formation was assessed in isolates from HH8-14 embryos (Fig. 6).

At HH8, olfactory precursors intermingle with lens and epidermal precursors (Bhattacharyya et al., 2004), precluding isolation of a homogenous population of nasal progenitors. Bearing this in mind, the explanted presumptive olfactory-lens region is both Pax6+ and Dlx3+ at 24 hours or 72 hours of culture (n=18/18) (Fig. 6A-A″). Interestingly, this ectoderm shows spatially segregated zones of gene expression, with the Dlx3+ cell cluster at one end of the explant (Fig. 6A) and Pax6+ cells at the other, forming a lentoid-like structure (Fig. 6A′, arrowhead). Pax6+/Dlx3+ cells are found at the intersection of the two domains (Fig. 6A″, arrows). This cell sorting is reminiscent of Dlx3 and Pax6 expression in the presumptive placodal region at HH13 (Fig. 3D″). Consistent with the possibility that placodal development in HH8 explants cannot progress beyond this stage in vitro, neither thickening nor neuronal differentiation were observed in these explants even after 3 days (Fig. 6A-A″) (Bailey et al., 2006). Although this appears contradictory to the findings of Sjodal et al. (Sjodal et al., 2007) where over 10% of cells in HH8 olfactory explants were keratin+/Hu+, these explants also expressed neural markers such as L5, HuC/D and Nkx2.1 in a distinct region. Similarly, in our hands, ~11% of ectodermal cells in HH8 explants were Hu+ when cultured with the anterior neural ridge (Bailey et al., 2006). By HH10, after olfactory and lens precursors have separated (Bhattacharyya et al., 2004), nasal progenitors are specified to express Dlx3 and Pax6 (n=20/20) and 20% of these explants differentiate to give rise to neurons (Fig. 6B,C,C′). Although Dlx3+ neurons can be unambiguously assigned to an olfactory fate (Fig. 6B, arrow), Dlx3– neurons (Fig. 6B, arrowhead) could either be olfactory (Fig. 3G) or forebrain-derived, as a few forebrain cells could have been explanted along with prospective placode. The segregation of Dlx3+, Pax6+ and Dlx3+/Pax6+ zones continues (Fig. 6C′). Although some explants exhibit thickening (Fig. 6C,C′), most contain cell aggregates with no particular structure. However, prospective nasal placode explanted at the cusp of thickening (HH13-14; n=25) forms a thickened epithelium and undergoes significant neurogenesis (Fig. 6D,E). Cumulatively, these results suggest that nasal placode precursors are specified to express Dlx3 and Pax6 as early as HH8; however, neuronal specification, as assayed by Hu expression, is noted only once nasal precursors have completely segregated from neighboring ectodermal populations and is complete just prior to acquiring placodal identity.

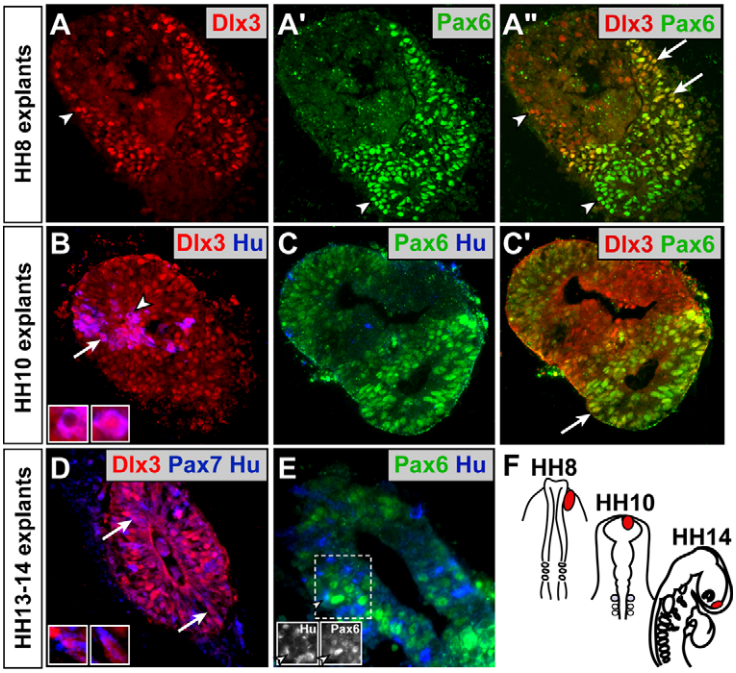

Fig. 6. Olfactory progenitors are specified to form neurons by HH10; placodal morphology is recapitulated in culture from HH13-14. (**A-A″**) Dlx3 (red) and Pax6 (green) are robustly expressed in HH8 explants; ~1/3 cells co-express both (arrows, A″, yellow); non-overlapping Dlx3 (A,A″, arrowhead) or Pax6 (A′,A″, arrowhead) domains appear distinct. (**B**) HH10 explant with neuronal differentiation; most neurons are Dlx3+/Hu+ (arrow), though some are Dlx3– (arrowhead). Insets show high-magnification views. (**C**) In HH10 explants, most cells are Pax6+ and few are Hu+ neurons. (**C′**) Arrow indicates cluster of Dlx3+/Pax6+ cells. Dlx3+ and Pax6+ cells segregate from double-positive cells. (**D**) Olfactory placode explanted at HH13 undergoes thickening in culture and has some Dlx3+/Hu+ (red/blue) cells (arrows, insets). Pax7 (blue, distinguishable from Hu by nuclear localization) delineates nasal mesenchyme underlying olfactory placode. (**E**) Newly thickened placodal ectoderm shows robust neuronal differentiation (Hu+, blue); some neurons are Pax6+ (green; arrowheads; insets). (**F**) Location of olfactory precursors at HH8, HH10 and HH14 based on fate maps.

Placodal precursors commit to olfactory fate concomitant with acquisition of placodal morphology at HH14

Operationally, a tissue is considered intrinsically committed to its fate if it recapitulates that fate when challenged by transplantation to a novel embryonic environment. As a rigorous test to determine irreversible commitment of olfactory placode ectoderm, its developmental potential was challenged by grafting it in place of non-placode forming trunk ectoderm. To this end, presumptive olfactory placode ectoderm derived from HH8-16 was transplanted to lateral plate ectoderm at the level of the most recently formed somites in HH8-9 chicks (Fig. 7A-C′). Even at HH8, grafts were committed to express Pax6 and Dlx3, paralleling their specification status (Fig. 7D). However, only a single graft from this stage expressed Hu, suggesting that neurogenesis was not yet fixed in most cases. At HH10, close apposition of the presumptive olfactory placode ectoderm with the forebrain makes their separation difficult. However, we cleanly dissected placodal ectoderm away from the forebrain in a few cases. The results show that, by HH10, olfactory precursors are not only capable of expressing Pax6/Dlx3 when grafted to the trunk, but a few graft-derived cells even differentiate as Hu+ neurons (Fig. 7E). We next heterotopically grafted older ectoderm (HH13) just prior to its thickening to form a morphologically distinct olfactory placode. In all cases, adherent mesenchyme was grafted with the presumptive placode ectoderm to the ectoderm overlying the lateral plate mesoderm. In two out of seven cases, the presumptive placodal ectoderm (identified by both Pax6 and Dlx3 expression) underwent thickening to acquire morphology characteristic of the olfactory placode and neuronal differentiation as assayed by Hu staining (Fig. 7F,F′). Isolated neurons appeared to migrate towards the dorsal aorta (Fig. 7F,F′, arrowheads). In the remaining five out of seven cases, no donor-derived neurons were detected. In these cases, although some of the grafted quail cells looked ectodermal and are Dlx3+/Pax6+, the majority of grafted cells appeared mesenchymal.

When placodal ectoderm is grafted (HH14-15; n=4), the ectoderm maintains its morphology, expresses Dlx3 and Pax6, and shows robust neuronal differentiation (Fig. 7G-G″). Interestingly, neurons that ingress from placodal ectoderm at this stage form a coherent group unlike grafts taken from younger donors (compare Fig. 7F,F′,G′,G″). Furthermore, graft-derived neurons are never found migrating through the Pax7+ mesenchyme, consistent with the endogenous situation where Hu+ cells migrate out of the olfactory epithelium in close association with each other and skirt the Pax7+ mesenchyme.

Cumulatively, our data suggest that once olfactory precursors segregate away from other ectodermal and placodal precursors, they are committed to express Dlx3 and Pax6 but have not yet received all signals for neuronal differentiation. Shortly before acquiring placodal morphology, transplanted olfactory ectoderm can express olfactory markers and differentiate; however, the neurons that ingress are not cohesive. Once the olfactory placode has acquired its characteristic morphology, differentiation occurs normally.

DISCUSSION

Olfactory progenitors arise within the anterior neural folds and adjacent ectoderm where they intermingle with lens precursors (Bhattacharyya et al., 2004). We have previously demonstrated that olfactory induction requires inhibition of lens fate by FGF at neurula stages and subsequently by signal(s) from the neural crest (Bailey et al., 2006). Here, we explore the spatiotemporal framework within which olfactory progenitors are precisely and reproducibly generated from an apparently homogenous field of anterior ectoderm. To this end, we define intrinsic properties of cranial ectoderm precursors that result in eventual irreversible acquisition of olfactory fate by a subset of these cells.

Molecular identity of developing olfactory placodes

Comparing fate maps and gene expression patterns enables identification of molecular markers that foreshadow olfactory fate. Using this approach, we identified three transcription factors, Dlx3, Dlx5 and Pax6, the combinatorial expression of which uniquely demarcates progenitors of the chick olfactory epithelium. Current literature suggests significant species-specific differences in the co-expression of Dlx3, Dlx5 and Pax6 in the olfactory epithelium. For

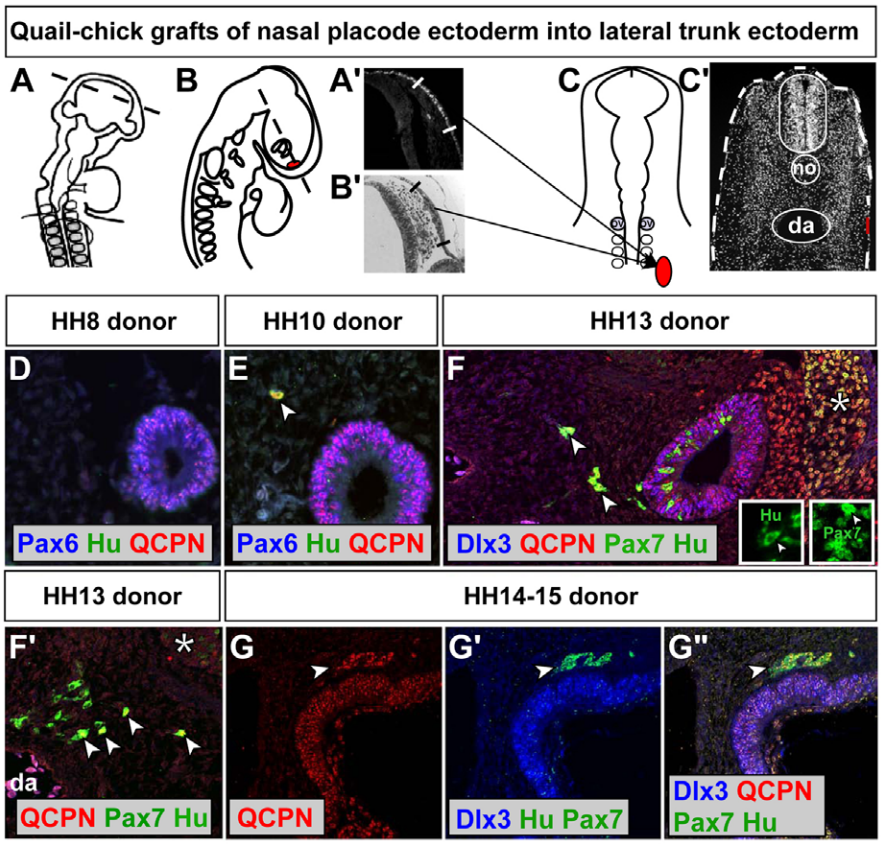

Fig. 7. Commitment towards olfactory fate occurs concomitant with acquisition of placodal morphology. (**A**) Schematic of HH13 quail embryo. Broken line indicates plane of section in A′. (**A′**) Section through prospective olfactory placode; white lines indicate grafted ectoderm overlying lateral plate (see C). (**B**) Schematic of HH14-15 quail embryo; broken line indicates plane of section in B′. (**B′**) Ultra-thin section through olfactory placode (courtesy of Dr John Sechrist, Caltech). (**C**) Red oval indicates placodal ectoderm grafted over lateral plate mesoderm. (**C′**) In section, broken white lines outline host trunk ectoderm and the red line indicates transplanted ectoderm. no, notochord; da, dorsal aorta. (**D**) Grafted HH8 ectoderm expresses Pax6 but not Hu. (**E**) Grafted HH10 ectoderm expresses Pax6 and forms few neurons (arrowhead). (**F**,**F′**) Grafts of HH13 ectoderm, thicken and differentiate as Hu+ neurons (cytoplasmic green); some are Dlx3+. Neurons delaminate and ingress, migrating in loose association (F,F′, arrowheads), some reaching the dorsal aorta (da). Pax7+ (nuclear green, asterisk) marks quail mesenchymal cells grafted with the presumptive placode (F) and host dermamyotome (F′). Pax7 and Hu show no expression overlap in these sections. (**G-G″**) Grafts of thickened placodal ectoderm (HH14-15) express Dlx3 (blue) and Pax6 (not shown), invaginate and morphologically resemble an endogenous olfactory pit. Arrowheads indicate Hu+ neurons that ingress from the placode and migrate as a chain. No Pax7+ cells were detected in this graft.

example, Dlx3 expression in the mouse is undetectable at E8.5 and only weakly detectable by E9.5 (Quint et al., 2000) or at E14.5 (Merlo et al., 2007), but appears to be conserved between chick and zebrafish (Akimenko et al., 1994; Ellies et al., 1997). By contrast, the expression pattern of Dlx5 is consistent between chick, mouse and frog (Papalopulu and Kintner, 1993; Pera et al., 1999; Yang et al., 1998); interestingly, Dlx5 expression is not observed in the gastrula stage zebrafish embryo and is detected only when olfactory precursors coalesce to form the placode (Akimenko et al., 1994; Ellies et al., 1997; Quint et al., 2000). Pax6 is expressed in the mouse (Grindley et al., 1995; Walther and Gruss, 1991), zebrafish (Krauss et al., 1991; Nornes et al., 1998; Puschel et al., 1992) and frog developing olfactory placodes (Franco et al., 2001), although a detailed timeline of its placodal expression is missing in the zebrafish.

These transcription factors not only serve as markers for developing nasal placodes, but also have functional importance. We show that some ingressing olfactory placode cells are Dlx+ and can become GnRH neurons. This is similar to the situation in mouse, where ~70% of the Dlx5+ cells become GnRH+ neurons that line the olfactory nerve (Merlo et al., 2007). In Dlx5 knockout mice, GnRH neuroendocrine cells persist but are mislocalized and express GnRH at reduced levels (Merlo et al., 2007). Dlx5-null mice have greatly reduced olfactory epithelia, with few sensory neurons therein, and rudimentary vomeronasal organs in addition to grossly impaired otic vesicle derivatives (Depew et al., 1999; Long et al., 2003; Merlo et al., 2007). Similarly, nasal placodes and cavities are absent in *small eye* (*Sey*) mice and rats lacking Pax6 (Fujiwara et al., 1994; Grindley et al., 1995; Hogan et al., 1986; Matsuo et al., 1993). Chimeric analysis shows a cell-autonomous requirement for Pax6 for full contribution to the lens and nasal epithelium (Collinson et al., 2000; Collinson et al., 2003); Pax6 appears to be required for the transition from nasal ectoderm to placode (Grindley et al., 1995). Likewise, in the zebrafish deletion mutant, b380, which lacks Dlx3a and Dlx3b, there is no induction of otic or olfactory placodes (Solomon and Fritz, 2002).

Origin of GnRH neuroendocrine cells

Evidence from mouse and chick supports an olfactory placode origin for basal forebrain localized GnRH neurons (Wray, 2002). In both organisms, detailed immunocytochemical analysis revealed GnRH+

cells in the olfactory epithelium, later along the olfactory nerve and finally in the forebrain (Murakami et al., 1991; Norgren and Lehman, 1991; Sullivan and Silverman, 1993; Wray et al., 1989a; Wray et al., 1989b). Furthermore, birth-dating forebrain GnRH neurons suggests they leave the mitotic cycle shortly before GnRH expression is seen in the olfactory epithelium (Mulrenin et al., 1999; Schwanzel-Fukuda and Pfaff, 1989; Wray et al., 1989a). More direct evidence for an olfactory placode origin for these neurons have come from dye labeling (Murakami and Arai, 1994), transplantation (Yamamoto et al., 1996) and ablation studies (Akutsu et al., 1992; Norgren and Gao, 1994). However, it has been argued that cells with non-olfactory placode origins could have mixed in with olfactory placode cells in these studies (Whitlock, 2008). Additional evidence in support of an olfactory placode origin has come from analysis of the *Sey* mutant, which lacks olfactory placodes and has no GnRH neurons (Dellovade et al., 1998; Skynner et al., 1999). Contrary to these studies, unilateral ablation of ectoderm immediately adjacent to, but not including, the olfactory placode at an early stage resulted in loss of forebrain-localized GnRH neurons (el Amraoui and Dubois, 1993).

Advanced teleost fishes (atherinomorpha, percomorpha), including zebrafish, have two distinct types of forebrain GnRH neurons: terminal nerve ganglia GnRH neurons and hypothalamic GnRH neurons (Parhar, 2002; Whitlock et al., 2003). Of these, the terminal nerve ganglia GnRH neurons were considered to originate from olfactory placode (von Bartheld and Baker, 2004). However, recent dye labeling and lineage analysis in zebrafish suggest that these neurons are neural crest derived (Whitlock et al., 2003). Furthermore, a severe reduction in the number of hypothalamic GnRH neurons was observed in the *you-too* mutant, which lacks most of the pituitary but has normal olfactory placodes (Whitlock et al., 2003). Our data are consistent with the hypothesis that at least some GnRH neurons in the forebrain region are olfactory placode ectoderm derived. However, we cannot rule out the possibility that other GnRH neurons might originate from embryonic populations such as the adenohypophyseal placode or the neural crest.

Spatiotemporal competence of ectoderm to form olfactory placode

Induction of structures at predetermined locations can occur by restricted localization of inducing signals and/or strict delimitation of responding tissue. For trigeminal placodes, dorsal neural tube at all axial levels have inducing ability, but competence to respond is relegated to cranial ectoderm (Baker et al., 1999). The converse occurs for otic placodes where inducing signals are localized at r2-7 while competence to respond is broad (Groves and Bronner-Fraser, 2000). Work from many laboratories suggests that growth-factors such as Fgf8, Bmp4, Shh and retinoic acid are crucial for induction of the olfactory placode (Bailey et al., 2006; Bhasin et al., 2003; Calof et al., 2002; Kawauchi et al., 2005; LaMantia et al., 2000). Accordingly, competence to co-express Pax6/Dlx3 and differentiate as olfactory cells is restricted and decreases steadily in an anterior-posterior gradient, with trunk ectoderm possessing negligible capacity to contribute to the nasal placode. Additionally, we find good correlation between the loss in competence to express olfactory markers and commitment to differentiate as other derivatives. For example, ability to express Pax6 is lost in grafts of HH10+ hindbrain level ectoderm as it is committed to an otic placode fate (Groves and Bronner-Fraser, 2000).

In comparing chick trigeminal, otic and olfactory placode competence (Baker et al., 1999; Groves and Bronner-Fraser, 2000) (and this study), trunk ectoderm has either no capacity to form placodes or only briefly retains this ability. Consistent with this, cranial ectoderm expresses epibranchial placode markers in response to BMP7 from pharyngeal endoderm but trunk ectoderm does not do so (Begbie et al., 1999). Competence to form lens is also restricted to lateral and ventral head ectoderm in amphibians and aves (Jacobson, 1966; Sullivan et al., 2004). In *Amblystoma punctatum*, as in chick, competence to form olfactory placode extends, at early stages, over a wide area of head ectoderm, but not to anterior flank ectoderm after stage 15 (Haggis, 1956). Furthermore, misexpression of signaling molecules or transcription factors involved in placodal development usually results in a partial recapitulation of the placode developmental program adjacent to the endogenous placodal territory or placodes forming in conjunction with neural tissue (Altmann et al., 1997; Barembaum and Bronner-Fraser, 2007; Begbie et al., 1999; Köster et al., 2000; Ladher et al., 2000; Taylor and Labonne, 2005; Vendrell et al., 2000). No experimental manipulation has so far led to the de novo generation of sensory or neurogenic placodes at all axial levels in the trunk ectoderm.

Recently, Martin and Groves (Martin and Groves, 2006) suggested a two-step model of placode induction wherein cranial ectoderm must first acquire generic properties of the pre-placodal region before responding to more specific placode-inducing signals. Wnt signals from lateral/posterior mesoderm and within trunk ectoderm have been hypothesized to restrict placode formation to a horseshoe-shaped domain in cranial ectoderm; however, Wnt inhibition alone cannot induce ectopic pre-placodal markers (Litsiou et al., 2005). Instead, intermediate levels of Bmp and Wnt inhibition in conjunction with Fgf signaling elicit pre-placodal markers such as Six1 and Six4 (Ahrens and Schlosser, 2005; Brugmann et al., 2004; Litsiou et al., 2005). Thus, signaling pathways can prime cranial but not trunk ectoderm to respond to placode-inducing cues.

Induction is complete before placodal morphogenesis

The capacity of presumptive olfactory ectoderm to express Pax6/Dlx3 and form neurons was assayed in 3D collagen gels. We find that presumptive olfactory placode ectoderm is specified to express Pax6 and Dlx3 by HH8 (Bailey et al., 2006) (this paper). Neuronal specification begins around HH10-11, implying that ectoderm has seen signals that will direct its fate even before it is morphologically visible as a placode, analogous to trigeminal, otic and lens placode specification (Baker et al., 1999; Groves and Bronner-Fraser, 2000; Sullivan et al., 2004).

We also determined the time when presumptive olfactory placode ectoderm is irreversibly committed by challenging its fate in a new environment via grafting over lateral plate ectoderm of HH8-9 chick embryos. Distant from the endogenous placode, this site probably lacks inducing signals. Interestingly, commitment to express Pax6 and Dlx3 and form some neurons occurred by HH10, before the placode is self-evident, consistent with early experiments showing that grafts of the anterior tip of HH11 embryos to the chorioallantoic membrane or trunk produced relatively normal olfactory organs in a small percentage of grafts (Street, 1937). However, sustained olfactory development only occurred once the placode acquired its characteristic morphology (Street, 1937). In *Amblystoma punctatum*, there is some discrepancy regarding when olfactory determination occurs. Although one study corroborates our findings (Haggis, 1956), another observes commitment to an olfactory fate at neurula stages (Carpenter, 1937). One possibility is that neural tissue was present in grafts of olfactory precursors taken at neurula stages, which would then continue to provide signals necessary for growth

and differentiation. Another possibility suggests that the site of transplantation might have been in range of olfactory-inducing stimuli (Haggis, 1956).

Conclusion

We show that co-expression of Dlx3, Dlx5 and Pax6 demarcates olfactory precursors prior to acquiring placodal status. Competence to form olfactory placode resides within head ectoderm up until HH9-10, but is largely absent from trunk ectoderm. Olfactory fate specification and commitment are complete just before acquiring overt placodal morphology and prior to differentiation into olfactory epithelium. This may highlight a general trend in placodal development.

We thank Drs Andy Groves and Michael Kessel for cDNA clones, Dr Jhumku Kohtz for the pan-Dlx antibody, Dr James Millam for the chick GnRH-I antibody, Dr Andy Kowalczyk for use of his microscope, and Matt Jones, David Arce and Andrea Manzo for technical assistance. We are grateful to Dr Tatjana Sauka-Spengler for critical reading of the manuscript and to Dr Andrea Streit for many helpful discussions. This work was supported by DE16459 to M.B.-F. and partly by a HHMI Predoctoral Fellowship to S.B.

References

Ahrens, K. and Schlosser, G. (2005). Tissues and signals involved in the induction of placodal Six1 expression in Xenopus laevis. *Dev. Biol.* **288**, 40-59.
Akimenko, M. A., Ekker, M., Wegner, J., Lin, W. and Westerfield, M. (1994). Combinatorial expression of the three zebrafish genes related to Distal-less: part of a homeobox gene code for the head. *J. Neurosci.* **14**, 3475-3486.
Akutsu, S., Takada, M., Ohki-Hamazaki, H., Murakami, S. and Arai, Y. (1992). Origin of luteinizing hormone-releasing hormone (LHRH) neurons in the chick embryo: effect of the olfactory placode ablation. *Neurosci Lett.* **142**, 241-244.
Altmann, C. R., Chow, R. L., Lang, R. A. and Hemmati-Brivanlou, A. (1997). Lens induction by Pax-6 in Xenopus laevis. *Dev. Biol.* **185**, 119-123.
Bailey, A. P. and Streit, A. (2006). Sensory organs: making and breaking the pre-placodal region. *Curr. Top. Dev. Biol.* **72**, 167-204.
Bailey, A. P., Bhattacharyya, S., Bronner-Fraser, M. and Streit, A. (2006). Lens specification is the ground state of all sensory placodes, from which FGF promotes olfactory identity. *Dev. Cell* **11**, 505-517.
Baker, C. V. H. and Bronner-Fraser, M. (2001). Vertebrate cranial placodes. Part I: embryonic induction. *Dev. Biol.* **232**, 1-61.
Baker, C. V., Stark, M. R., Marcelle, C. and Bronner-Fraser, M. (1999). Competence, specification and induction of Pax-3 in the trigeminal placode. *Development* **126**, 147-156.
Baker, H. and Margolis, F. L. (2002). Mechanisms of differentiation and migration of olfactory progenitors: an overview. *Chem. Senses* **27**, 567.
Balmer, C. W. and LaMantia, A. S. (2005). Noses and neurons: induction, morphogenesis, and neuronal differentiation in the peripheral olfactory pathway. *Dev. Dyn.* **234**, 464-481.
Barembaum, M. and Bronner-Fraser, M. (2007). Spalt4 mediates invagination and otic placode gene expression in cranial ectoderm. *Development* **134**, 3805-3814.
Beanan, M. J. and Sargent, T. D. (2000). Regulation and function of Dlx3 in vertebrate development. *Dev. Dyn.* **218**, 545-553.
Begbie, J., Brunet, J. F., Rubenstein, J. L. and Graham, A. (1999). Induction of the epibranchial placodes. *Development* **126**, 895-902.
Bhasin, N., Maynard, T. M., Gallagher, P. A. and LaMantia, A. S. (2003). Mesenchymal/epithelial regulation of retinoic acid signaling in the olfactory placode. *Dev. Biol.* **261**, 82-98.
Bhattacharyya, S., Bailey, A. P., Bronner-Fraser, M. and Streit, A. (2004). Segregation of lens and olfactory precursors from a common territory: cell sorting and reciprocity of Dlx5 and Pax6 expression. *Dev. Biol.* **271**, 403-414.
Brown, S. T., Martin, K. and Groves, A. K. (2003). Molecular basis of inner ear induction. *Curr. Top. Dev. Biol.* **57**, 115-149.
Brown, S. T., Wang, J. and Groves, A. K. (2005). Dlx gene expression during chick inner ear development. *J. Comp. Neurol.* **483**, 48-65.
Brugmann, S. A., Pandur, P. D., Kenyon, K. L., Pignoni, F. and Moody, S. A. (2004). Six1 promotes a placodal fate within the lateral neurogenic ectoderm by functioning as both a transcriptional activator and repressor. *Development* **131**, 5871-5881.
Calof, A. L., Mumm, J. S., Rim, P. C. and Shou, J. (1998). The neuronal stem cell of the olfactory epithelium. *J. Neurobiol.* **36**, 190-205.
Calof, A. L., Bonnin, A., Crocker, C., Kawauchi, S., Murray, R. C., Shou, J. and Wu, H. H. (2002). Progenitor cells of the olfactory receptor neuron lineage. *Microsc. Res. Tech.* **58**, 176-188.
Carpenter, E. (1937). The head pattern in Ambystoma studied by vital staining and transplantation methods. *J. Exp. Zool.* **75**, 103-129.
Chow, R. L. and Lang, R. A. (2001). Early eye development in vertebrates. *Annu. Rev. Cell Dev. Biol.* **17**, 255-296.
Chuah, M. I. and West, A. K. (2002). Cellular and molecular biology of ensheathing cells. *Microsc. Res. Tech.* **58**, 216-227.
Collinson, J. M., Hill, R. E. and West, J. D. (2000). Different roles for Pax6 in the optic vesicle and facial epithelium mediate early morphogenesis of the murine eye. *Development* **127**, 945-956.
Collinson, J. M., Quinn, J. C., Hill, R. E. and West, J. D. (2003). The roles of Pax6 in the cornea, retina, and olfactory epithelium of the developing mouse embryo. *Dev. Biol.* **255**, 303-312.
Couly, G. F. and Le Douarin, N. M. (1985). Mapping of the early neural primordium in quail-chick chimeras. I. Developmental relationships between placodes, facial ectoderm, and prosencephalon. *Dev. Biol.* **110**, 422-439.
Couly, G. and Le Douarin, N. M. (1990). Head morphogenesis in embryonic avian chimeras: evidence for a segmental pattern in the ectoderm corresponding to the neuromeres. *Development* **108**, 543-558.
D'Amico-Martel, A. and Noden, D. M. (1983). Contributions of placodal and neural crest cells to avian cranial peripheral ganglia. *Am. J. Anat.* **166**, 445-468.
Davis, J. A. and Reed, R. R. (1996). Role of Olf-1 and Pax-6 transcription factors in neurodevelopment. *J. Neurosci.* **16**, 5082-5094.
Dellovade, T. L., Pfaff, D. W. and Schwanzel-Fukuda, M. (1998). The gonadotropin-releasing hormone system does not develop in Small-Eye (Sey) mouse phenotype. *Brain Res. Dev. Brain Res.* **107**, 233-240.
Depew, M. J., Liu, J. K., Long, J. E., Presley, R., Meneses, J. J., Pedersen, R. A. and Rubenstein, J. L. (1999). Dlx5 regulates regional development of the branchial arches and sensory capsules. *Development* **126**, 3831-3846.
Depew, M. J., Simpson, C. A., Morasso, M. and Rubenstein, J. L. (2005). Reassessing the Dlx code: the genetic regulation of branchial arch skeletal pattern and development. *J. Anat.* **207**, 501-561.
Dhawan, R. R., Schoen, T. J. and Beebe, D. C. (1997). Isolation and expression of homeobox genes from the embryonic chicken eye. *Mol. Vis.* **3**, 7.
Donner, A. L., Lachke, S. A. and Maas, R. L. (2006). Lens induction in vertebrates: variations on a conserved theme of signaling events. *Semin. Cell Dev. Biol.* **17**, 676-685.
Dulac, C. (1997). Molecular biology of pheromone perception in mammals. *Semin. Cell Dev. Biol.* **8**, 197-205.
Eisenstat, D. D., Liu, J. K., Mione, M., Zhong, W., Yu, G., Anderson, S. A., Ghattas, I., Puelles, L. and Rubenstein, J. L. (1999). DLX-1, DLX-2, and DLX-5 expression define distinct stages of basal forebrain differentiation. *J. Comp. Neurol.* **414**, 217-237.
el Amraoui, A. and Dubois, P. M. (1993). Experimental evidence for an early commitment of gonadotropin-releasing hormone neurons, with special regard to their origin from the ectoderm of nasal cavity presumptive territory. *Neuroendocrinology* **57**, 991-1002.
Ellies, D. L., Stock, D. W., Hatch, G., Giroux, G., Weiss, K. M. and Ekker, M. (1997). Relationship between the genomic organization and the overlapping embryonic expression patterns of the zebrafish dlx genes. *Genomics* **45**, 580-590.
Fernandez-Garre, P., Rodriguez-Gallardo, L., Gallego-Diaz, V., Alvarez, I. S. and Puelles, L. (2002). Fate map of the chicken neural plate at stage 4. *Development* **129**, 2807-2822.
Firnberg, N. and Neubüser, A. (2002). FGF signaling regulates expression of Tbx2, Erm, Pea3, and Pax3 in the early nasal region. *Dev. Biol.* **247**, 237-250.
Fornaro, M., Geuna, S., Fasolo, A. and Giacobini-Robecchi, M. G. (2001). Evidence of very early neuronal migration from the olfactory placode of the chick embryo. *Neuroscience* **107**, 191-197.
Fornaro, M., Geuna, S., Fasolo, A. and Giacobini-Robecchi, M. G. (2003). HuC/D confocal imaging points to olfactory migratory cells as the first cell population that expresses a post-mitotic neuronal phenotype in the chick embryo. *Neuroscience* **122**, 123-128.
Franco, M. D., Pape, M. P., Swiergiel, J. J. and Burd, G. D. (2001). Differential and overlapping expression patterns of X-dll3 and Pax-6 genes suggest distinct roles in olfactory system development of the African clawed frog Xenopus laevis. *J. Exp. Biol.* **204**, 2049-2061.
Fujiwara, M., Uchida, T., Osumi-Yamashita, N. and Eto, K. (1994). Uchida rat (rSey): a new mutant rat with craniofacial abnormalities resembling those of the mouse Sey mutant. *Differentiation* **57**, 31-38.
Garcia-Martinez, V., Alvarez, I. S. and Schoenwolf, G. C. (1993). Locations of the ectodermal and nonectodermal subdivisions of the epiblast at stages 3 and 4 of avian gastrulation and neurulation. *J. Exp. Zool.* **267**, 431-446.
Grainger, R. M. (1992). Embryonic lens induction: shedding light on vertebrate tissue determination. *Trends Genet.* **8**, 349-355.
Graziadei, G. A. and Graziadei, P. P. (1979). Neurogenesis and neuron regeneration in the olfactory system of mammals. II: degeneration and reconstitution of the olfactory sensory neurons after axotomy. *J. Neurocytol.* **8**, 197-213.
Graziadei, P. P. and Metcalf, J. F. (1971). Autoradiographic and ultrastructural observations on the frog's olfactory mucosa. *Z. Zellforsch. Mikrosk. Anat.* **116**, 305-318.

Graziadei, P. P. and Monti Graziadei, A. G. (1983). Regeneration in the olfactory system of vertebrates. *Am. J. Otolaryngol.* **4**, 228-233.
Grindley, J. C., Davidson, D. R. and Hill, R. E. (1995). The role of Pax-6 in eye and nasal development. *Development* **121**, 1433-1442.
Groves, A. K. and Bronner-Fraser, M. (2000). Competence, specification and commitment in otic placode induction. *Development* **127**, 3489-3499.
Haggis, A. J. (1956). Analysis of the determination of the olfactory placode in ambystoma punctatum. *J. Embryol. Exp. Morphol.* **4**, 120-138.
Hogan, B. L., Horsburgh, G., Cohen, J., Hetherington, C. M., Fisher, G. and Lyon, M. F. (1986). Small eyes (Sey): a homozygous lethal mutation on chromosome 2 which affects the differentiation of both lens and nasal placodes in the mouse. *J. Embryol. Exp. Morphol.* **97**, 95-110.
Jacobson, A. G. (1966). Inductive processes in embryonic development. *Science* **125**, 25-34.
Kawauchi, S., Shou, J., Santos, R., Hebert, J. M., McConnell, S. K., Mason, I. and Calof, A. L. (2005). Fgf8 expression defines a morphogenetic center required for olfactory neurogenesis and nasal cavity development in the mouse. *Development* **132**, 5211-5223.
Köster, R. W., Kuhnlein, R. P. and Wittbrodt, J. (2000). Ectopic Sox3 activity elicits sensory placode formation. *Mech. Dev.* **95**, 175-187.
Krauss, S., Johansen, T., Korzh, V., Moens, U., Ericson, J. U. and Fjose, A. (1991). Zebrafish pax[zf-a]: a paired box-containing gene expressed in the neural tube. *EMBO J.* **10**, 3609-3619.
Ladher, R. K., Anakwe, K. U., Gurney, A. L., Schoenwolf, G. C. and Francis-West, P. H. (2000). Identification of synergistic signals initiating inner ear development. *Science* **290**, 1965-1967.
LaMantia, A. S., Bhasin, N., Rhodes, K. and Heemskerk, J. (2000). Mesenchymal/epithelial induction mediates olfactory pathway formation. *Neuron* **28**, 411-425.
Litsiou, A., Hanson, S. and Streit, A. (2005). A balance of FGF, BMP and WNT signalling positions the future placode territory in the head. *Development* **132**, 4051-4062.
Liu, J. K., Ghattas, I., Liu, S., Chen, S. and Rubenstein, J. L. (1997). Dlx genes encode DNA-binding proteins that are expressed in an overlapping and sequential pattern during basal ganglia differentiation. *Dev. Dyn.* **210**, 498-512.
Long, J. E., Garel, S., Depew, M. J., Tobet, S. and Rubenstein, J. L. (2003). DLX5 regulates development of peripheral and central components of the olfactory system. *J. Neurosci.* **23**, 568-578.
Martin, K. and Groves, A. K. (2006). Competence of cranial ectoderm to respond to Fgf signaling suggests a two-step model of otic placode induction. *Development* **133**, 877-887.
Matsuo, T., Osumi-Yamashita, N., Noji, S., Ohuchi, H., Koyama, E., Myokai, F., Matsuo, N., Taniguchi, S., Doi, H., Iseki, S. et al. (1993). A mutation in the Pax-6 gene in rat small eye is associated with impaired migration of midbrain crest cells. *Nat. Genet.* **3**, 299-304.
Megason, S. G. and McMahon, A. P. (2002). A mitogen gradient of dorsal midline Wnts organizes growth in the CNS. *Development* **129**, 2087-2098.
Merlo, G. R., Mantero, S., Zaghetto, A. A., Peretto, P., Paina, S. and Gozzo, M. (2007). The role of Dlx homeogenes in early development of the olfactory pathway. *J. Mol. Histol.* **38**, 347-358.
Mulrenin, E. M., Witkin, J. W. and Silverman, A. J. (1999). Embryonic development of the gonadotropin-releasing hormone (GnRH) system in the chick: a spatio-temporal analysis of GnRH neuronal generation, site of origin, and migration. *Endocrinology* **140**, 422-433.
Murakami, S. and Arai, Y. (1994). Direct evidence for the migration of LHRH neurons from the nasal region to the forebrain in the chick embryo: a carbocyanine dye analysis. *Neurosci. Res.* **19**, 331-338.
Murakami, S., Seki, T., Wakabayashi, K. and Arai, Y. (1991). The ontogeny of luteinizing hormone-releasing hormone (LHRH) producing neurons in the chick embryo: possible evidence for migrating LHRH neurons from the olfactory epithelium expressing a highly polysialylated neural cell adhesion molecule. *Neurosci. Res.* **12**, 421-431.
Noramly, S. and Grainger, R. M. (2002). Determination of the embryonic inner ear. *J. Neurobiol.* **53**, 100-128.
Norgren, R. B., Jr and Lehman, M. N. (1991). Neurons that migrate from the olfactory epithelium in the chick express luteinizing hormone-releasing hormone. *Endocrinology* **128**, 1676-1678.
Norgren, R. B., Jr and Gao, C. (1994). LHRH neuronal subtypes have multiple origins in chickens. *Dev. Biol.* **165**, 735-738.
Nornes, S., Clarkson, M., Mikkola, I., Pedersen, M., Bardsley, A., Martinez, J. P., Krauss, S. and Johansen, T. (1998). Zebrafish contains two pax6 genes involved in eye development. *Mech. Dev.* **77**, 185-196.
Northcutt, R. G. and Muske, L. E. (1994). Multiple embryonic origins of gonadotropin-releasing hormone (GnRH) immunoreactive neurons. *Brain Res. Dev. Brain Res.* **78**, 279-290.
Osumi-Yamashita, N., Ninomiya, Y., Doi, H. and Eto, K. (1994). The contribution of both forebrain and midbrain crest cells to the mesenchyme in the frontonasal mass of mouse embryos. *Dev. Biol.* **164**, 409-419.
Panganiban, G. and Rubenstein, J. L. (2002). Developmental functions of the Distal-less/Dlx homeobox genes. *Development* **129**, 4371-4386.
Panganiban, G., Sebring, A., Nagy, L. and Carroll, S. (1995). The development of crustacean limbs and the evolution of arthropods. *Science* **270**, 1363-1366.
Papalopulu, N. and Kintner, C. (1993). Xenopus Distal-less related homeobox genes are expressed in the developing forebrain and are induced by planar signals. *Development* **117**, 961-975.
Parhar, I. S. (2002). Cell migration and evolutionary significance of GnRH subtypes. *Prog. Brain Res.* **141**, 3-17.
Pera, E. and Kessel, M. (1999). Expression of DLX3 in chick embryos. *Mech. Dev.* **89**, 189-193.
Pera, E., Stein, S. and Kessel, M. (1999). Ectodermal patterning in the avian embryo: epidermis versus neural plate. *Development* **126**, 63-73.
Price, M. (1993). Members of the Dlx- and Nkx2-gene families are regionally expressed in the developing forebrain. *J. Neurobiol.* **24**, 1385-1399.
Puschel, A. W., Gruss, P. and Westerfield, M. (1992). Sequence and expression pattern of pax-6 are highly conserved between zebrafish and mice. *Development* **114**, 643-651.
Quint, E., Zerucha, T. and Ekker, M. (2000). Differential expression of orthologous Dlx genes in zebrafish and mice: implications for the evolution of the Dlx homeobox gene family. *J. Exp. Zool.* **288**, 235-241.
Ramon-Cueto, A. and Avila, J. (1998). Olfactory ensheathing glia: properties and function. *Brain Res. Bull.* **46**, 175-187.
Riley, B. B. and Phillips, B. T. (2003). Ringing in the new ear: resolution of cell interactions in otic development. *Dev. Biol.* **261**, 289-312.
Robinson, G. W. and Mahon, K. A. (1994). Differential and overlapping expression domains of Dlx-2 and Dlx-3 suggest distinct roles for Distal-less homeobox genes in craniofacial development. *Mech. Dev.* **48**, 199-215.
Rosenquist, G. C. (1966). A radioautographic study of labeled grafts in the chick blastoderm. In *Contributions to Embryology*. Vol. 38, pp. 73-110. Washington: Carnegie Institution.
Saha, M. S., Spann, C. L. and Grainger, R. M. (1989). Embryonic lens induction: more than meets the optic vesicle. *Cell Differ. Dev.* **28**, 153-171.
Sambrook, J. and Russell, D. W. (2001). *Molecular Cloning: A Laboratory Manual*. 3rd edn. Cold Spring Harbor, NY: Cold Spring Harbor Laboratory Press.
Schlosser, G. (2006). Induction and specification of cranial placodes. *Dev. Biol.* **294**, 303-351.
Schoenwolf, G. C. and Alvarez, I. S. (1991). Specification of neurepithelium and surface epithelium in avian transplantation chimeras. *Development* **112**, 713-722.
Schwanzel-Fukuda, M. and Pfaff, D. W. (1989). Origin of luteinizing hormone-releasing hormone neurons. *Nature* **338**, 161-164.
Serbedzija, G. N., Bronner-Fraser, M. and Fraser, S. E. (1992). Vital dye analysis of cranial neural crest cell migration in the mouse embryo. *Development* **116**, 297-307.
Sjodal, M., Edlund, T. and Gunhaga, L. (2007). Time of exposure to BMP signals plays a key role in the specification of the olfactory and lens placodes *ex vivo*. *Dev. Cell* **13**, 141-149.
Skynner, M. J., Slater, R., Sim, J. A., Allen, N. D. and Herbison, A. E. (1999). Promoter transgenics reveal multiple gonadotropin-releasing hormone-I-expressing cell populations of different embryological origin in mouse brain. *J. Neurosci.* **19**, 5955-5966.
Solomon, K. S. and Fritz, A. (2002). Concerted action of two dlx paralogs in sensory placode formation. *Development* **129**, 3127-3136.
Stark, M. R., Sechrist, J., Bronner-Fraser, M. and Marcelle, C. (1997). Neural tube-ectoderm interactions are required for trigeminal placode formation. *Development* **124**, 4287-4295.
Street, S. F. (1937). The differentiation of the nasal area of the chick embryo in grafts. *J. Exp. Zool.* **77**, 49-80.
Streit, A. (2001). Origin of the vertebrate inner ear: evolution and induction of the otic placode. *J. Anat.* **199**, 99-103.
Streit, A. (2002). Extensive cell movements accompany formation of the otic placode. *Dev. Biol.* **249**, 237-254.
Streit, A. and Stern, C. D. (2001). Combined whole-mount in situ hybridization and immunohistochemistry in avian embryos. *Methods* **23**, 339-344.
Sullivan, C. H., Braunstein, L., Hazard-Leonards, R. M., Holen, A. L., Samaha, F., Stephens, L. and Grainger, R. M. (2004). A re-examination of lens induction in chicken embryos: in vitro studies of early tissue interactions. *Int. J. Dev. Biol.* **48**, 771-782.
Sullivan, K. A. and Silverman, A. J. (1993). The ontogeny of gonadotropin-releasing hormone neurons in the chick. *Neuroendocrinology* **58**, 597-608.
Tarozzo, G., Peretto, P. and Fasolo, A. (1995). Cell migration from the olfactory placode and the ontogeny of the neuroendocrine compartments. *Zool. Sci.* **12**, 367-383.
Taylor, K. M. and Labonne, C. (2005). SoxE factors function equivalently during neural crest and inner ear development and their activity is regulated by SUMOylation. *Dev. Cell* **9**, 593-603.
Torres, M. and Giraldez, F. (1998). The development of the vertebrate inner ear. *Mech. Dev.* **71**, 5-21.
van Wijhe, J. W. (1883). Uber die Mesodermsegmente und die Entwicklung der Nerven des Selachierkopfes. *Verhandelingen der Koninklijke Akademie van Wetenschappen (Amsterdam)* **22**(**E**), 1-50.

Vendrell, V., Carnicero, E., Giraldez, F., Alonso, M. T. and Schimmang, T. (2000). Induction of inner ear fate by FGF3. *Development* **127**, 2011-2019.
von Bartheld, C. S. and Baker, C. V. (2004). Nervus terminalis derived from the neural crest? A surprising new turn in a century-old debate. *Anat. Rec. B New Anat.* **278**, 12-13.
von Kupffer, C. (1891). The development of the cranial nerves of vertebrates. *J. Comp. Neurol.* **1**, 246-264; 315-332.
Walther, C. and Gruss, P. (1991). Pax-6, a murine paired box gene, is expressed in the developing CNS. *Development* **113**, 1435-1449.
Whitlock, K. E. (2005). Origin and development of GnRH neurons. *Trends Endocrinol. Metab.* **16**, 145-151.
Whitlock, K. E. (2008). Developing a sense of scents: plasticity in olfactory placode formation. *Brain Res. Bull.* **75**, 340-347.
Whitlock, K. E. and Westerfield, M. (2000). The olfactory placodes of the zebrafish form by convergence of cellular fields at the edge of the neural plate. *Development* **127**, 3645-3653.
Whitlock, K. E., Wolf, C. D. and Boyce, M. L. (2003). Gonadotropin-releasing hormone (GnRH) cells arise from cranial neural crest and adenohypophyseal regions of the neural plate in the zebrafish, Danio rerio. *Dev. Biol.* **257**, 140-152.
Wilson, S. I., Rydstrom, A., Trimborn, T., Willert, K., Nusse, R., Jessell, T. M. and Edlund, T. (2001). The status of Wnt signalling regulates neural and epidermal fates in the chick embryo. *Nature* **411**, 325-330.
Wray, S. (2002). Development of gonadotropin-releasing hormone-1 neurons. *Front. Neuroendocrinol.* **23**, 292-316.
Wray, S., Grant, P. and Gainer, H. (1989a). Evidence that cells expressing luteinizing hormone-releasing hormone mRNA in the mouse are derived from progenitor cells in the olfactory placode. *Proc. Natl. Acad. Sci. USA* **86**, 8132-8136.
Wray, S., Nieburgs, A. and Elkabes, S. (1989b). Spatiotemporal cell expression of luteinizing hormone-releasing hormone in the prenatal mouse: evidence for an embryonic origin in the olfactory placode. *Brain Res. Dev. Brain Res.* **46**, 309-318.
Xu, H., Dude, C. M. and Baker, C. V. (2008). Fine-grained fate maps for the ophthalmic and maxillomandibular trigeminal placodes in the chick embryo. *Dev. Biol.* **317**, 174-186.
Yamamoto, N., Uchiyama, H., Ohki-Hamazaki, H., Tanaka, H. and Ito, H. (1996). Migration of GnRH-immunoreactive neurons from the olfactory placode to the brain: a study using avian embryonic chimeras. *Brain Res. Dev. Brain Res.* **95**, 234-244.
Yang, L., Zhang, H., Hu, G., Wang, H., Abate-Shen, C. and Shen, M. M. (1998). An early phase of embryonic Dlx5 expression defines the rostral boundary of the neural plate. *J. Neurosci.* **18**, 8322-8330.
Zhu, H. and Bendall, A. J. (2006). Dlx3 is expressed in the ventral forebrain of chicken embryos: implications for the evolution of the Dlx gene family. *Int. J. Dev. Biol.* **50**, 71-75.